Multi-period vulnerability analysis of power grids under multiple outages: An AC-based bilevel optimization approach

Abedi, Amin; Romerio-Giudici, Franco

How to cite

ABEDI, Amin, ROMERIO-GIUDICI, Franco. Multi-period vulnerability analysis of power grids under multiple outages: An AC-based bilevel optimization approach. In: International Journal of Critical Infrastructure Protection, 2020, n° 100365. doi: 10.1016/j.ijcip.2020.100365

This publication URL: https://archive-ouverte.unige.ch//unige:139637
Publication DOI: 10.1016/j.ijcip.2020.100365

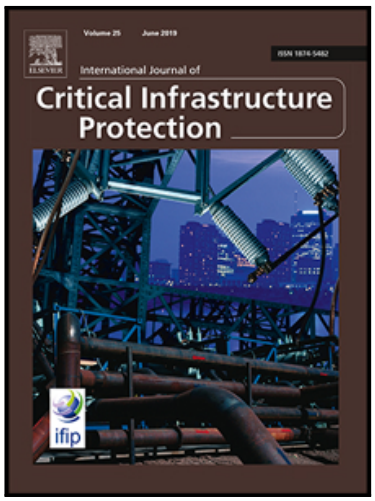

Multi-period vulnerability analysis of power grids under multiple outages: An AC-based bilevel optimization approach

Amin Abedi , Franco Romerio

PII: S1874-5482(20)30029-9
DOI: https://doi.org/10.1016/j.ijcip.2020.100365
Reference: IJCIP 100365

To appear in: *International Journal of Critical Infrastructure Protection*

Received date: 22 October 2019
Revised date: 3 June 2020
Accepted date: 19 July 2020

Please cite this article as: Amin Abedi , Franco Romerio , Multi-period vulnerability analysis of power grids under multiple outages: An AC-based bilevel optimization approach, *International Journal of Critical Infrastructure Protection* (2020), doi: https://doi.org/10.1016/j.ijcip.2020.100365

Multi-period vulnerability analysis of power grids under multiple outages: An AC-based bilevel optimization approach

Amin Abedi[*]*, Franco Romerio*

Institute for Environmental Sciences, University of Geneva, Switzerland

Abstract-

This paper describes a methodology for the *N-k* contingency analysis of bulk power systems. The method encompasses the evaluation of contingencies' effects on the power system over a range of system demand levels. The proposed model is inherently a multi-period bilevel optimization problem. Unlike the conventional bilevel optimization problems for the *N-k* contingency analysis, the proposed model considers the effects of reactive power dispatch, losses, and voltage profile. In doing so, the problem is formulated as a multi-period AC-based bilevel mixed-integer nonlinear programming (MINLP) problem. To guarantee the global optimality of the solution, this paper linearizes and then transforms it into a one-level mixed-integer linear programming (MILP) problem using different linearization techniques and the duality theory. The simulation results on the annual load profile of the IEEE Reliability Test System (RTS) verify the effectiveness of the proposed model.

Keywords- *N-k* contingency analysis, bilevel MINLP, Stackelberg game approach, power system.

Nomenclature

Indices

i,j	Indices of buses
kc	Index of regular polygon for linearizing the circle
l	Index of lines
m	Index of blocks used for piecewise linearization

Sets

D	Set of all buses with a demand
G	Set of all buses with a generation
L	Set of all lines
NB	Set of all buses
T	Set of time (days or hours)

Constants

B	Big *M* parameter
c_i	cost coefficients of generators ($/MWh)
k	Number of outages (interdiction resources)
M	Number of blocks used for piecewise linearization
n	Number of sides of a regular polygon to formulate a circle
N	Number of assets
$Pg_i^{\max}$	Maximum magnitude of active power of generators at bus *i* (MW)
$Qg_i^{\max}$	Maximum magnitude of reactive power of generators at bus *i* (MVAR)
$Qg_i^{\min}$	Minimum magnitude of reactive power of generators at bus *i* (MVAR)
R(l)	Receiving bus of line *l*
S(l)	Sending bus of line *l*
$S_{ij}^{\max}$	Maximum magnitude of apparent power of line *ij* (MVA)
$V_i^{\max}$	Maximum magnitude of voltage magnitude at bus *i* (V)
$V_i^{\min}$	Minimum magnitude of voltage magnitude at bus *i* (V)
Y_{ij}	Admittance of line *ij* $(Y_{ij} = G_{ij} + jB_{ij})$
$\theta_{ij}^{\max}$	Maximum of voltage angle difference between bus *i* and *j* (Rad)
$\theta_{ij}^{\min}$	Minimum of voltage angle difference between bus *i* and *j* (Rad)
$\Delta\theta_{ij}$	Maximum of each block width for line *ij*

Variables

H_l, T_l	Two sets of continuous variables to linearize the product of binary and continuous dual variables
Ls_i^t	Active power load shedding at bus *i* (MW) in time *t*
Lsq_i^t	Reactive power load shedding at bus *i* (MVAR) in time *t*

P_{ij}^t	Active power flow of line *ij* (MW) in time *t*
Pg_i^t	Active power of generators at bus *i* (MW) in time *t*
Pd_i^t	Active power demand at bus *i* (MW) in time *t*
V_{it}	Voltage magnitude at bus *i* (V) in time *t*
Q_{ij}^t	Reactive power flow of line *ij* (MVAR) in time *t*
Qg_i^t	Reactive power of generators at bus *i* (MVAR) in time *t*
Qd_i^t	Reactive power demand at bus *i* (MVAR) in time *t*
Z / z_l^t	Upper level decision variable / Binary variable in time t that is equal to 0 if line *l* is out of service and otherwise, is equal to *1*
θ_{ijt}	Voltage angle difference between bus *i* and *j* (Rad) in time *t*
θ_{ijm}	Width of the mth angle block of line *ij* (Rad)
$\delta_{ij}^+, \delta_{ij}^-$	Positive variables used to eliminate the absolute function
$\lambda_{ij}, \mu_{ij}, \alpha_i, \overline{\omega}_i,$ $\beta_i, \overline{\delta}_i, \overline{\sigma}_i, \overline{\upsilon}_i, \xi_{ij},$ $\underline{\upsilon}_i, \eta_{1,ij} \cdots \eta_{n,ij}, \chi_{ij},$ $o_{ijm}, \varphi_{ij}, \kappa_{ijm}, \varepsilon_{ij}$	Dual variables that are shown on top of the corresponding equalities or inequalities

1. Introduction

Energy is a vital commodity in modern societies and power systems play a crucial role in providing secure and reliable energy. Protection of the power system as a critical infrastructure against different hazards and threats i.e., natural hazards, intentional attacks, and random failures [1] has become a growing concern. Furthermore, the interdependencies between power systems and communication networks in smart grids are introducing new challenges i.e., cyber threats. So, the operators and planners must protect the most vulnerable elements of a system under a variety of attack scenarios in order to improve the system security and deploying a robust and resilient power system [2].

In this context, a key question is which components are critical and must be protected or fortified when the protective and financial resources are limited [3]. To this end, it is fundamental to develop robust methodologies and tools to assess the vulnerability of a power system against external attacks [4]. Hence, the vulnerability analysis and, in particular, prioritizing the vulnerable components result in an effective power system protection with limited resources [5].

Contingency analysis or *N-k* contingency assessment is a methodology looking for a set of *k* critical components of the power system whose simultaneous failure would maximize the damage, in terms of the amount of involuntary load shedding in the power system. *N-k* (

$k \geq 2$) contingencies are low-probability events but inherently more severe than *N*-1 contingencies in triggering cascading failures and even blackouts [6]. Therefore, the North American Reliability Council (NERC) suggests power system planners and operators considering *N*-*k* contingency analysis in their planning and operation [7]. The difficulty of *N*-*k* contingency selection is that it follows the combination formula. It means that for a very modest size power system with *N*=1000, there are 1000 '*N*-1' contingencies, 499500 '*N*-2' contingencies, over 160 million '*N*-3' contingencies, over 40 billion '*N*-4' contingencies and so on. So, the number of possible *N*-*k* contingencies, even for small values of *k*, makes total enumeration approaches computationally impractical in a large-scale interconnected power network [8].

Scientists have been developing innovative methods to determine critical components whose failures lead to the largest system loss. Generally, there are two different lines of work in the literature. Some literature work on the low-order contingencies including single or a small number of component failures that have a very high occurrence probability. For instance, the *N*-1 security constraint that all of the regulatory agencies in the world enforce the system operators to satisfy it by strict security standards. Within this constraint, the system should normally continue to work after any single failure [9]. Analyzing the loss of two elements consecutively or *N*-1-1 contingency analysis is another example of this category [10-12]. It should be noted that the reliability concept that defines the ability of the electric power system to meet the demand with continuity and an acceptable level of quality, comes under the low-order contingencies [13].

The second line of works presents not only the low-order but also the high-order contingencies. The high-order contingencies include a relatively large number of component failures that have a very low occurrence probability but high consequences. The focus of this paper is on this type of assessment i.e. the vulnerability analysis of power systems. The vulnerability can be social, organizational, economic, environmental, territorial, physical, and systemic [14, 15]. Most studies focus on physical and systemic vulnerabilities. Physical vulnerability represents the degree of loss of an element due to external pressure such as natural hazards [16]. In contrast, systemic vulnerability considers the degree of redundancy, functionality, and dependency of a system due to the failure of a specific element or an interconnected system [17]. This paper aims to investigate the behavior of the power system i.e. systemic vulnerability to identify the critical components under a worst-case scenario such as an intentional attack.

The works can range from analytical approaches (complex network, flow-based, logical, and functional methods) to Monte Carlo simulations. A detailed comparison of these approaches is recently conducted in [18] (and the references therein). Among them, the optimization-based problem can directly lead to promising results without the need to rank the sets of critical assets. The application of these approaches is considerably increasing in the complex problems thanks to the advent of advanced high-speed multiprocessors with large memory. It makes the problem tractable for a realistic power system [19].

The interdiction model is at the forefront of the models used to identify the worst *N*-*k* contingency. It has been developed based on a multilevel optimization problem to assess the vulnerability of power systems [20]. A multilevel optimization is a mathematical program

where an optimization problem contains another optimization problem as a constraint [21]. These problems are also known as the hierarchical leader-follower problem or the Stackelberg game [22]. The interdiction model basically includes an upper level whose objective is to identify exactly *k* components to maximize the damage (load shedding) in the system and a lower level whose objective is mitigating the impacts of attacks and minimizing the damage consequences.

Later, the interdiction model is developed based on two models i.e., bilevel and trilevel interdiction models. For instance, Karush-Kuhn-Tucker (KKT) optimality conditions [23] and duality theory [24] are used to convert a bilevel attacker-defender model to a one-level problem. Arroyo J.M. [25] compared the KKT- and duality-based approaches by introducing minimum and maximum vulnerability models. Brown et al. [26] extended the classical bilevel interdiction model to a general trilevel defender-attacker-defender model to assign limited defensive resources in power systems. Alguacil et al. [27] proposed an approach to allocate the defensive resources in a power system to mitigate the vulnerability. Wu et al [28] decomposed a planner-attacker-operator model to a master problem and a subproblem using a Benders primal decomposition method. Recently, Fang et al. [29, 30] and Che et al. [31] used this approach to identify the vulnerability of power grids exposed to natural hazards and the hidden *N-k* contingencies, respectively and finally, Nemati et al. [32, 33] proposed tri-level transmission expansion planning (TTEP) under physical intentional attacks.

The above-surveyed literature uses the simplified formulation of nonlinear AC optimal power flow (ACOPF) i.e., the DC optimal power flow (DCOPF) as the lower level. The DCOPF has some drawbacks. Technically, it cannot provide precise information on the power system since it ignores reactive power, resistance and losses and fixes the voltage values for the buses. Mathematically, restricting the available degrees of freedom (e.g., fixed voltages in DC-based method) makes the solution non-optimal and less accurate [34].

To the best of our knowledge, a few studies considered a real picture of the power grid parameters i.e. both active and reactive powers, losses, and voltage profile to assess the vulnerability of the power system. Kim et al. [35] used the AC power flow equations and the Frank Wolfe algorithm to compute an optimal solution of the problem. However, they assumed that attackers are allowed to increase the impedance of transmission lines in the model. Modeling component removal needs to introduce binary variables that require different and more complicated solution techniques. Recently, a probabilistic *N-k* model is introduced to analyze a probabilistic generalization of the interdiction model using the cutting-plane algorithm [8]. They use convex relaxations instead of the DC power flow approximation.

Generally speaking, the ACOPF is a non-linear and non-convex optimization problem [19] which is used as the lower level in this paper. Considering the ACOPF for each time period (*t*) as the lower level converts the problem to a bilevel mixed-integer nonlinear programming (MINLP) problem that is very complicated and challenging to solve. It should be emphasized that employing metaheuristic algorithms or non-linear solvers does not guarantee to have a global optimum solution [36]. The aim of this paper is to tackle the new problem and avoid the probable local solution for each time period (*t*). The contributions of the proposed model in this paper are threefold:

(1) A novel deterministic multi-period AC-based one-level MILP formulation of a bilevel MINLP problem is introduced so as to assess the *N-k* contingency analysis.

(2) The model considers a real picture of the power grid parameters i.e., both active and reactive powers, losses, and voltage profile.

(3) The planners can decide the level of accuracy by setting the predefined parameters (i.e., *n* and *M*) that are introduced in the linearization process for each time period (*t*).

The remainder of this paper is organized as follows. Section 2 introduces the multi-period AC-based bilevel MINLP problem. Section 3 proposes the solution approaches to linearize and then, transforming to a one-level MILP problem. Sections 4 and 5 present the test case and the numerical results, respectively. Discussions and concluding remarks are finally provided in sections 6 and 7, respectively.

2. The multi-period AC-based bilevel MINLP problem

In this section, the mathematical formulation of multi-period AC-based bilevel MINLP problem is introduced. The model provides the worst-case scenario under multiple outages that is of interest in *N-k* security assessment. This formulation is based on the following assumptions that are commonly used for vulnerability and contingency assessment of a power system [23-28, 37, 38]:

1- The rational attacker (the worst-case scenario) is considered trying to maximize the damage and can disable multiple assets simultaneously and permanently or at least for several hours. As a result, the power flow of other lines will be affected.
2- The power system has two main components i.e., substations or transmissions and transformers. Herein, the targeting assets are transmission lines and transformers, because they are usually reachable with low or no security to withstand. However, by removing the connected lines and transformers of a load bus, it will be spontaneously out of service.
3- Because two parallel circuits between the buses are usually on the same tower, they are modeled as a single line with double capacity. Furthermore, the shunt susceptances of the lines are ignored.
4- A steady-state security model and multi-period scenario are considered where typically, the highest load demand forecast is used in each time period (i.e., daily, hourly, etc.).
5- Herein, the system damage is load shedding, that is, the amount of involuntarily decreasing the load demand. In the lower level, we assumed the active and reactive loads are shed independently [39]. Admittedly, different objective functions as the system damage can be defined based on the interest.
6- The ratings of transmission lines are not only limited by the power flowing in that line but also they are dependent on the conductor material and radius and the weather such as solar irradiance, ambient temperature, wind speed, and wind direction. In the following formulation, a static thermal rating is used. However, applying the dynamic thermal rating in the model is also straightforward.

According to the multi-period interdiction (attacker-defender) model in Figure 1, the attacker as a leader or upper-level problem starts the game with the limited disruptive resources. The system operator as a follower or lower-level problem reacts against the set of out-of-service assets to mitigate its adverse consequences based on the following formulations whose dual variables are shown on top of the corresponding equalities or inequalities:

$$\underset{z}{Max} \sum_{i \in NB} Ls_i^{t^*} \tag{1}$$

Subject to:

$$0.5 \times \sum_{i,j \in N} (1 - z_{ij}{}^t) = k; \quad z_{ij}{}^t \in \{0,1\} \quad \forall i, j \in N \tag{2}$$

$$\sum_{i \in NB} Ls_i^{t^*} \in \arg \left\{ \underset{\substack{Pg,Qg,Ls,Lsq,\\ P,Q,V,\theta}}{Min} \sum_{i \in NB} Ls_i^t \right\} \tag{3}$$

Subject to:

$$Pg_{i|i \in D}^t + Ls_{i|i \in D}^t - Pd_{i|i \in D}^t \overset{\alpha_i}{=} \sum_{j \in NB} P_{ij}^t; \quad \forall i, j \in NB, \forall t \in T \tag{4}$$

$$Qg_{i|i \in G}^t + Lsq_{i|i \in D}^t - Qd_{i|i \in D}^t \overset{\beta_i}{=} \sum_{j \in NB} Q_{ij}^t; \quad \forall i, j \in NB, \forall t \in T \tag{5}$$

$$P_{ij}^t = z_l{}^t \left(V_{it}{}^2 G_{ij} - V_{it} V_{jt} (G_{ij} \cos \theta_{ijt} + B_{ij} \sin \theta_{ijt}) \right); \quad \forall l \in L, \forall t \in T \tag{6}$$

$$Q_{ij}^t = z_l{}^t \left(-V_{it}{}^2 B_{ij} - V_{it} V_{jt} (G_{ij} \sin \theta_{ijt} - B_{ij} \cos \theta_{ijt}) \right); \quad \forall l \in L, \forall t \in T \tag{7}$$

$$0 \le Pg_i^t \overset{\bar{\delta}_i}{\le} Pg_i^{\max}; \quad \forall i \in G, \forall t \in T \tag{8}$$

$$Qg_i^{\min} \overset{\underline{\sigma}_i}{\le} Qg_i^t \overset{\bar{\sigma}_i}{\le} Qg_i^{\max}; \quad \forall i \in G, \forall t \in T \tag{9}$$

$$\left(P_{ij}^t\right)^2 + \left(Q_{ij}^t\right)^2 \le \left(S_{ij}{}^{\max}\right)^2; \quad \forall l \in L, \forall t \in T \tag{10}$$

$$V_i{}^{\min} \overset{\underline{\upsilon}_i}{\le} V_{it} \overset{\bar{\upsilon}_i}{\le} V_i^{\max}; \quad \forall i \in NB, \forall t \in T \tag{11}$$

$$\theta_{ij}{}^{\min} \le \theta_{ijt} \le \theta_{ij}{}^{\max}; \quad \forall i, j \in NB, \forall t \in T \tag{12}$$

$$0 \le Ls_i^t \overset{\bar{\omega}_i}{\le} Pd_i^t; \quad \forall i \in D, \forall t \in T \tag{13}$$

$$0 \le Lsq_i^t \overset{\bar{\psi}_i}{\le} Qd_i^t; \quad \forall i \in D, \forall t \in T \tag{14}$$

Equation (1) shows the objective function that the attacker is trying to maximize with the constraint sets (2)-(14). Equation (2) is the upper-level constraint that shows the maximum number of outages (k) is fixed. If z_l is 0, the line l is under attack. Otherwise, it is safe. Moreover, note that factor 0.5 is multiplied by the total number of line outages because $z_l = z_{ij} = z_{ji}$ and the line ij is considered twice in the formulation. In the lower-level problem

(3)-(14), unlike the previous approaches [23-28], the ACOPF is used as the operator tool to mitigate the adverse consequences of the outages. Equation (3) is the objective of the system operator to minimize the damage. The asterisk in (1) and (3) emphasizes that Ls_i are decision variables of the lower level problem. Equations (4) and (5) are the nodal power balance equations for active and reactive powers, respectively. Equations (6) and (7) represent the line flows of active and reactive powers, respectively. Constraints (8)-(14) enforce the limits of active and reactive power generations, transmission line capacity, voltage, and voltage angle, active and reactive load shedding, respectively. The above-formulated problem is a bilevel MINLP problem due to the nonlinearities in equations (6),(7) and (10). In the following sections, just for the sake of simplicity, the superscript "*t*" has been dropped.

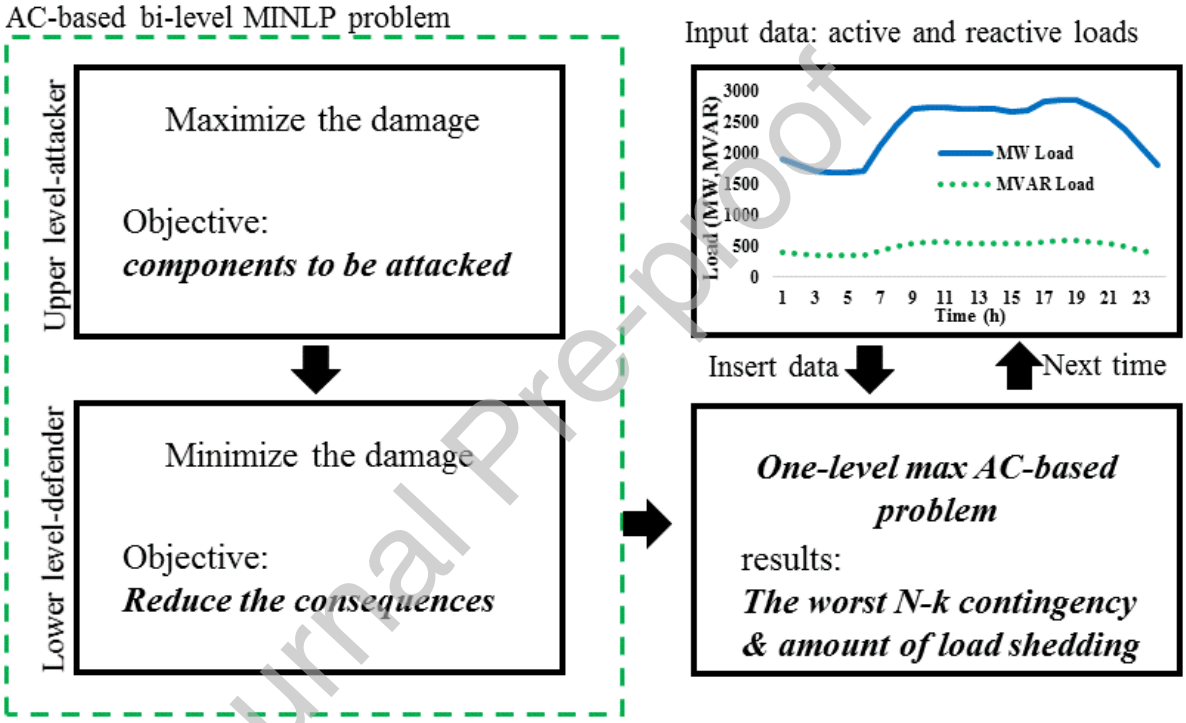

Figure 1. The multi-period AC-based bilevel MINLP problem.

3. Solution methodology

It should be noted that there will be no guarantee to obtain the global solution due to the non-convexity non-linearity nature of the proposed approach [40] with a non-linear solver or evolutionary approaches [19]. Therefore, we transformed it to one-level MILP problem in two steps. First, the lower-level problem is transformed to a MILP problem to avoid any local solution. Then, the duality theory [41] is used to have a one-level MILP problem in the second step.

3.1. Linearizing lower-level NLP problem

To linearize the lower-level NLP problem, the phase differences between the bus voltages are assumed small enough and the voltage magnitude is close to 1 p.u. for all buses. These

assumptions are practically acceptable under the normal operating condition to maintain the system far from instability [19]. Based on the aforementioned assumptions, the first-order approximation of Taylor's series with respect to the variables $\{V_i, V_j, \cos\theta_{ij}, \sin\theta_{ij}\}$ is used for nonlinear terms of equations (6)-(7) (z_l is a constant at this level). Then, the quadratic function is linearized based on the proposed method in [42] by using 2M piecewise linear (PWL) blocks as below:

$$P_{ij} \overset{\lambda_l}{=} z_l \left(G_{ij}\left(2V_i - 1\right) - G_{ij}\left(V_i + V_j + (1 - \frac{\sum_{m=1}^{M}((2m-1)\Delta\theta_{ij})\theta_{ijm}}{2}) - 2 \right) - B_{ij}(\delta_{ij}^{+} - \delta_{ij}^{-}) \right) \tag{15}$$

$$Q_{ij} \overset{\mu_l}{=} z_l \left(-B_{ij}\left(2V_i - 1\right) + B_{ij}\left(V_i + V_j + (1 - \frac{\sum_{m=1}^{M}((2m-1)\Delta\theta_{ij})\theta_{ijm}}{2}) - 2 \right) - G_{ij}(\delta_{ij}^{+} - \delta_{ij}^{-}) \right) \tag{16}$$

$$\left|\theta_i - \theta_j\right| = \sum_{m=1}^{M}\theta_{ijm} \overset{\varphi_{ij}}{=} \delta_{ij}^{+} + \delta_{ij}^{-}; \quad m = 1\cdots M, \forall i, j \in NB \tag{17}$$

$$0 \le \theta_{ijm} \overset{o_{ijm}}{\le} \Delta\theta_{ij}; \quad m = 1\cdots M, \forall i, j \in NB \tag{18}$$

$$\theta_{ijm} \overset{\kappa_{ijm}}{=} \theta_{jim}; \quad m = 1\cdots M, \forall i, j \in NB \tag{19}$$

Where, $(2m-1)\Delta\theta_{ij}$ and θ_{ijm} are the slope and the value of the m[th] block of the voltage phase difference of transmission line ij (see Figure 2). Derivation of equations (15) and (16) are described in the appendix. The appropriate value for $\Delta\theta_{ij}$ can be $\frac{\pi}{M}$. The absolute function in (17) is modeled by introducing two positive variables i.e., δ_{ij}^{+} and δ_{ij}^{-}. This linearization technique of the quadratic function doesn't need to have binary variables compared to other linearization techniques such as the binary expansion theory [43], the special ordered set of type 2 (SOS2) [36]. Nevertheless, this technique adds three sets of continuous variables to the problem (M+2 variables for each line). Adding binary variables change the lower-level problem to a MILP problem that is impossible to use the duality theory in the next step to have a one-level MILP problem [27].

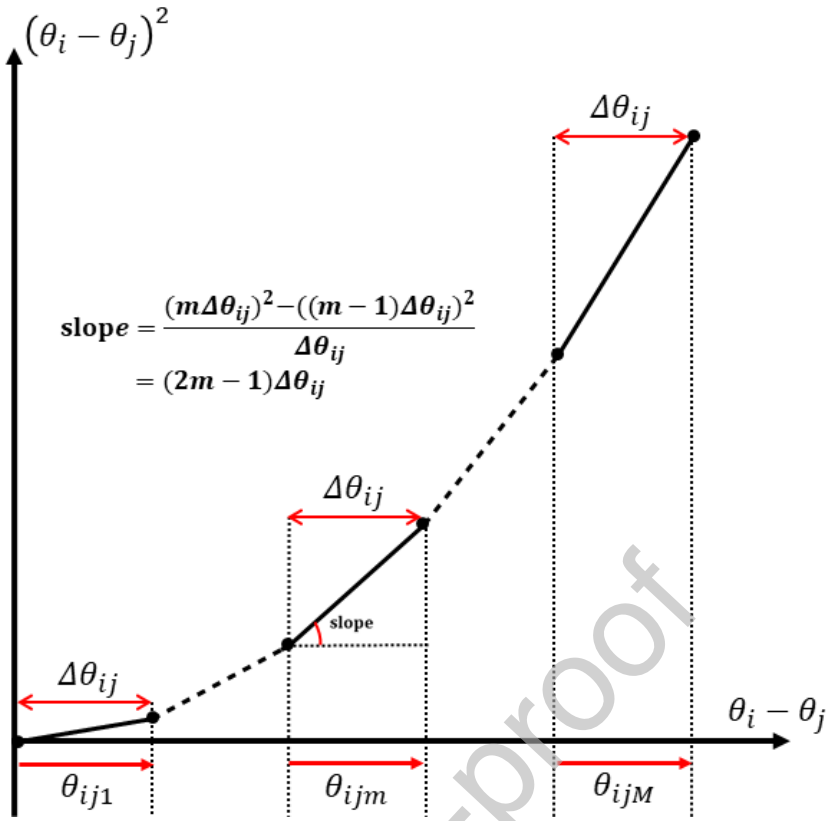

Figure 2. Piecewise linear approximation of a nonlinear function.

As can be seen, the last nonlinear constraint of the lower-level problem (i.e., equation (10)) presents a circle with the radius of $S_{ij}^{\max}$. This circle is linearized by an n-sided convex regular polygon using the following n equations [44]:

$$\left(\sin\left(\frac{2\pi kc}{n}\right)-\sin\left(\frac{2\pi(kc-1)}{n}\right)\right)P_{ij}-\left(\cos\left(\frac{2\pi kc}{n}\right)-\cos\left(\frac{2\pi(kc-1)}{n}\right)\right)Q_{ij}$$
$$-S_{ij}^{\max}\sin\left(\frac{2\pi}{n}\right)^{\eta_{k,l}}\leq 0;\quad kc=1\cdots n,\forall i,\ j\in NB \tag{20}$$

In fact, the linearization of (10) adds "n" equations for each line. A small n forces more restrictions on transmission line capacity and probably leads to the infeasible problem while a big n increases the number of equations and simulation time. The appropriate value for n can be 64 [19, 36]. Thereafter, the problem is completely a bilevel MILP which can be transformed into one-level MILP in the next section using the duality theory [41].

3.2. Transforming to an equivalent one-level MILP problem

The duality theory states that every linear programming (LP) problem (the primal problem) has another LP problem (the dual problem) that can be derived from it. The dual problem will be a maximization problem when the primal problem is a minimization problem and vice versa. Furthermore, each variable (constraint) in the primal problem becomes a constraint (variable) in the dual problem [41]. So, in order to transform the bilevel max-min problem to

a max-max problem, the duality theory is used below. Then, the max-max problem is reformulated to a one-level max problem as follows.

$$\underset{\substack{z_{ij},\lambda_{ij},\underline{\mu}_{ij},\underline{\alpha}_i,\overline{\omega}_i,\\ \beta_i,\overline{\delta}_i,\overline{\sigma}_i,\underline{\upsilon}_i,\underline{\xi}_{ij},\\ \underline{\upsilon}_i,\eta_{1,ij}\cdots\eta_{n,ij},\chi_{ij},\\ o_{ijm},\varphi_{ij},\kappa_{ijm},\varepsilon_{ij}}}{Max} \begin{pmatrix} \sum_{l\in L} z_l\lambda_l G_{ij} - \sum_{l\in L} z_l\mu_l B_{ij} + \sum_{i\in NB}(\alpha_i+\overline{\omega}_i)Pd_{i|i\in D} + \sum_{i\in NB}(\beta_i+\overline{\psi}_i)Qd_{i|i\in D} \\ +\sum_{i\in G}\overline{\delta}_i Pg_i^{\max} + \sum_{i\in G}\overline{\sigma}_i Qg_i^{\max} + \sum_{i\in G}\underline{\sigma}_i Qg_i^{\min} + \sum_{i\in NB}\overline{\upsilon}_i V_i^{\max} + \sum_{i\in NB}\underline{\upsilon}_i V_i^{\min} \\ +\sum_{l\in L} S_{ij}^{\max}\sin\left(\frac{2\pi}{n}\right)(\eta_{1,l}+\cdots+\eta_{n,l}) + \sum_{l\in L}\chi_{ij} + \sum_{l\in L}\sum_{m=1}^{M} o_{ijm}\Delta\theta_{ij} \end{pmatrix} \tag{21}$$

Subject to:

$$0.5\times\sum_{i,j\in N}(1-z_{ij}) = k;\quad z_{ij}\in\{0,1\}\quad \forall i,j\in N \tag{22}$$

$$\lambda_l - \alpha_i + \sum_{kc=1}^{n}\eta_{kc,l}\left(\sin\left(\frac{2\pi kc}{n}\right)-\sin\left(\frac{2\pi(kc-1)}{n}\right)\right)^{P_{ij}} = 0 \tag{23}$$

$$\mu_l - \beta_i - \sum_{kc=1}^{n}\eta_{kc,l}\left(\cos\left(\frac{2\pi kc}{n}\right)-\cos\left(\frac{2\pi(kc-1)}{n}\right)\right)^{Q_{ij}} = 0 \tag{24}$$

$$-\sum_{l|S(l)=i} z_l\lambda_l G_{ij} + \sum_{l|R(l)=i} z_l\lambda_l G_{ij} + \sum_{l|S(l)=i} z_l\mu_l B_{ij} - \sum_{l|R(l)=i} z_l\mu_l B_{ij} + \overline{\upsilon}_i + \underline{\upsilon}_i^{V_i} = 0 \tag{25}$$

$$z_l\lambda_l G_{ij} - z_l\mu_l B_{ij} + \chi_{ij}^{c_{ij}} = 0 \tag{26}$$

$$z_l\lambda_l B_{ij} + z_l\mu_l G_{ij} + \xi_{ij} + \varepsilon_{ij}^{\pi_{ij}} + \varepsilon_{ji} = 0 \tag{27}$$

$$\alpha_i + \overline{\delta}_i^{Pg_{i|i\in G}} \le 0 \tag{28}$$

$$\beta_i + \overline{\sigma}_i + \underline{\sigma}_i^{Qg_{i|i\in G}} = 0 \tag{29}$$

$$+\varphi_{ij} - \xi_{ij}^{\delta_{ij}^{+}} \le 0 \tag{30}$$

$$\varphi_{ij} + \xi_{ij}^{\delta_{ij}^{-}} \le 0 \tag{31}$$

$$\chi_{ij}(0.5(2m-1)\Delta\theta_{ij}) - \varphi_{ij} + o_{ijm} + \kappa_{ijm} - \kappa_{jim}^{\theta_{ijm}} \le 0 \tag{32}$$

$$\alpha_i + \overline{\omega}_i^{Ls_{i|i\in D}} \le 1 \tag{33}$$

$$\beta_i + \overline{\psi}_i^{Lsq_{i|i\in D}} \le 0 \tag{34}$$

Where the primal variables are shown on top of the corresponding equalities or inequalities. This transformation introduces a new nonlinearity to the model i.e., the product of binary and continuous dual variables ($z_l\lambda_l$ and $z_l\mu_l$) in equations (21), (25)-(27). This product can be

easily linearized using two sets of continuous variables T_l and H_l [27, 45] that is introduced in the appendix.

4. Test system

The IEEE Reliability Test System (RTS) and IEEE 57-bus are used in this paper. The IEEE 57-bus test case is only used for comparison. It represents a portion of the American Electric Power system (in the U.S. Midwest) and has 57 buses, 7 generators, and 42 loads [46]. Data availability makes the IEEE RTS an ideal test case for multi-period bulk power system vulnerability analysis. It contains 24 buses, 32 generators, and 38 branches (lines plus transformers) as shown in Figure 3. The transmission lines operate at two different voltage levels, 132 kV and 230 kV. The system working at 230 kV and 132 kV are represented in the upper half and the lower half of Figure 3, respectively. Detailed data of the systems can be found in [46, 47]. Furthermore, the annual load profile of the IEEE RTS is shown in Figure 4. This profile can be adapted to seasonal patterns. If the first week is assumed the first week of the calendar year, then the profile shows the annual peak occurring in the week prior to Christmas (winter). If the week number one is assumed to be the first week of August, then the annual peak will occur in the month of July (summer) [47].

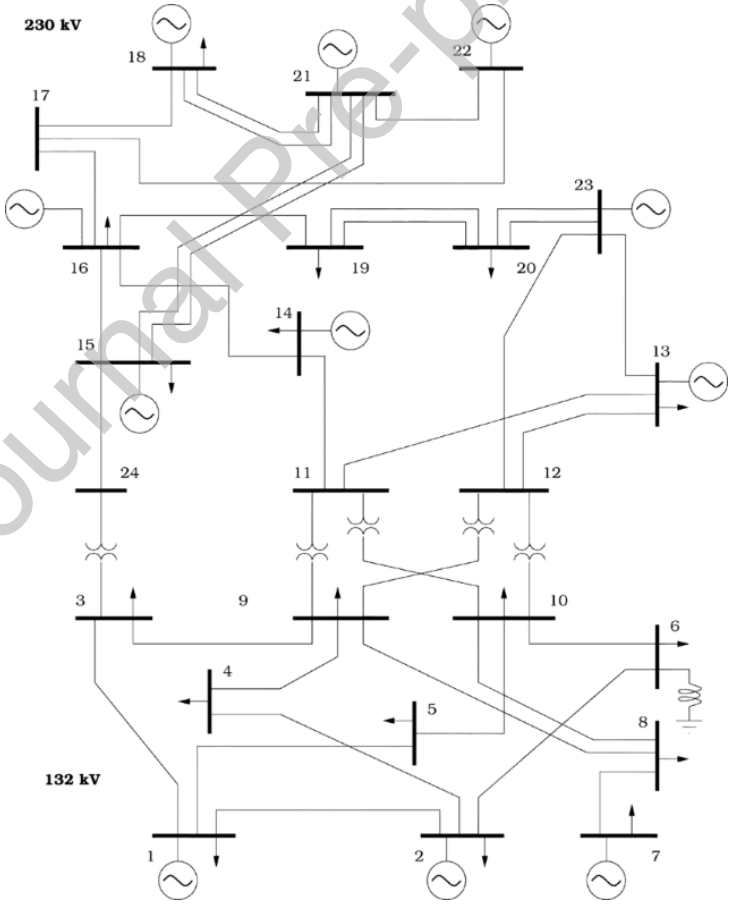

Figure 3. Topology of IEEE 24-bus reliability test systems (RTS).

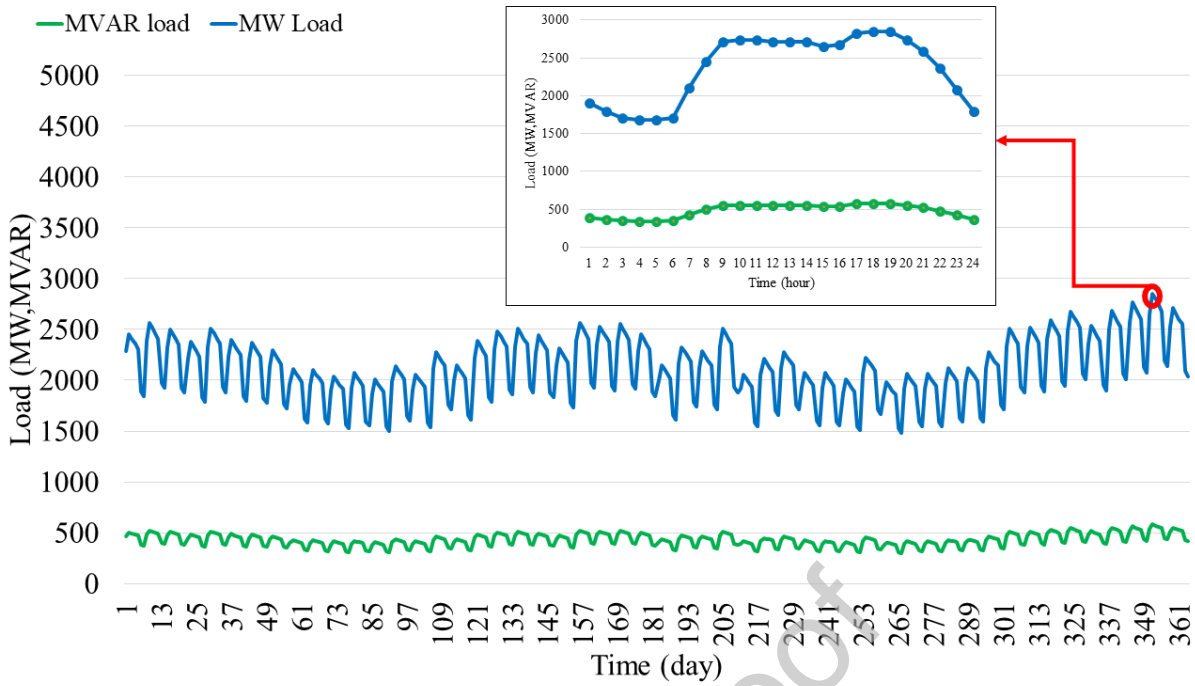

Figure 4. System daily peak loads in one year with highlighted annual peak load.

5. Numerical results

The proposed model has been successfully applied to the test systems. In this numerical study, the minimum and maximum of the voltage magnitude of buses are assumed to be 0.95 and 1.05 p.u., respectively [48]. The problems are solved on a laptop running with an Intel Core i7, 2.2 GHz processor, and 8 GB RAM. The CPLEX solver which uses the branch and cut algorithm is employed under GAMS (General Algebraic Modeling System) [49]. Furthermore, the ACOPF function of MATPOWER in MATLAB environment [48] is also used for comparing the results.

In linearization, it is assumed M=80 and n=64. Larger values for these parameters do not change the results [19, 36]. With these assumptions, Table 1 shows the comparison of statistic data for different test cases. It compares the average elapsed time of the models with the different numbers of nonzero elements, single equations, single variables, and binary variables. As discussed before, the difficulty of *N-k* contingency selection is that it follows the combination formula. Trendline of the simulation time shows that in the low-order contingencies and the orders that the objective function does not change afterward (e.g., k=13 in the IEEE RTS network), the simulation time is the minimum value while the number of samples is increasing (Figure 5).

Table 1. Comparison of statistic data of different test cases

Model statistics	IEEE 24-bus		IEEE 57-bus	
	DC-based	AC-based	DC-based	AC-based
Blocks of equations	12	25	12	25
Blocks of variables	12	87	12	87
Nonzero elements	1993	49300	4476	112781
Single equations	533	6684	1200	15289
Single variables	512	16153	1157	36994
Binary variables	68	68	156	156
Average elapsed time/simulation (min)	<1	~2	~4	~23

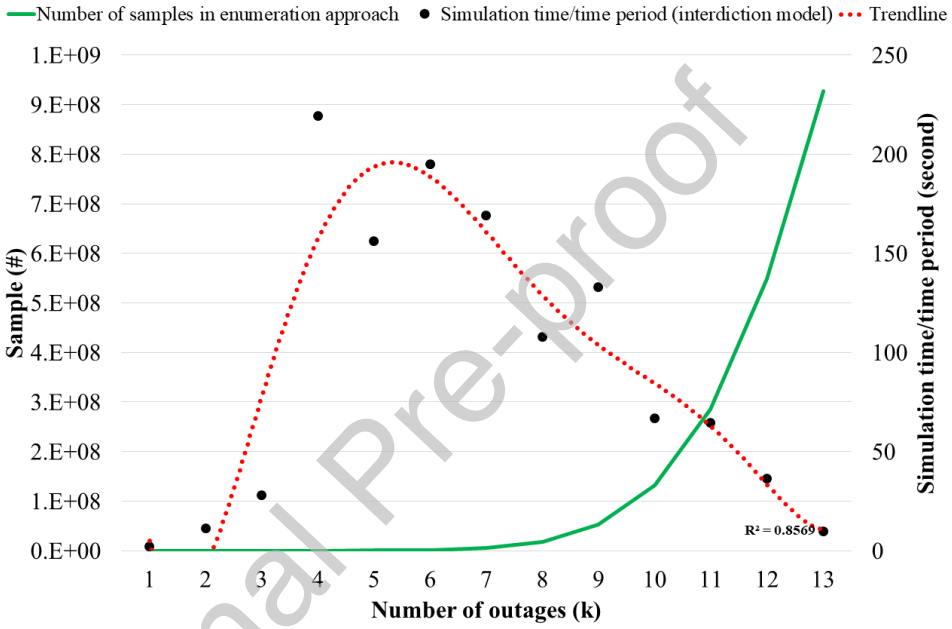

Figure 5. Comparing enumeration-based approach and this approach in the case of simulation time for the IEEE RTS network.

5.1. Accuracy of the lower-level problem and its strong duality

Before proceeding to implement the proposed method on the IEEE RTS network, the accuracy of the linearized ACOPF problem in the lower level and its dual problem are investigated. In doing so, the exact nonlinear ACOPF using MATPOWER package and proposed linearized ACOPF method are compared. The objective function for the ACOPF problem is introduced as the total operation cost of the generators in the form of $\sum_{i\in G} c_i Pg_i$ [48].

For the exact ACOPF and DCOPF models using MATPOWER package, the objective functions are 44196 $/h and 41904 $/h, respectively, whereas the objective function is found to be 44322 $/h using the lower-level problem in this paper. The results show an error of 5.2 % for the exact DC-OPF method and a very small error of 0.3 % for the linearized ACOPF in the lower-level problem. Furthermore, the objective function is found to be 44322 $/h using

its dual problem. This result demonstrates the strong duality in the problem where the optimal values of the primal and dual problems are equal [45].

5.2. Comparison between the proposed approach and the previous literature

The previous literature uses the DCOPF as the operator tool in the lower level problem whose objective is minimizing the damage consequences [23-28]. It means that the reactive power, variation of voltage magnitude, power losses, and the line resistance are ignored [50]. It also approximated the small angle. It considers that the differences of the voltage angle between the neighboring buses *i* and *j* are insignificant, that is, $\sin(\theta_{ij})\approx\theta_{ij}$ and $\cos(\theta_{ij})\approx1$ [51]. Hence, to derive the DC-based approach [23-28] for a fair comparison, the equations (1)-(14) are revised based on the above assumptions. So, equations (5), (7), (9), (11) and (14) are ignored and equations (6) and (10) are reformulated based on the assumptions.

Then, both models are applied to the test cases. The results show that small differences in total load sheddings, lead to proposing different critical lines in the IEEE RTS network. For instance, when *k* is 8, the proposed approach and the previous approach [23-28] find 6 similar critical lines (i.e., 7-8(l_{11}), 11-13(l_{18}), 12-13(l_{20}), 15-21(l_{25}, l_{26}), 16-17(l_{28}), 20-23(l_{36}, l_{37})) while they propose different lines (1-5(l_3), 12-23(l_{21})) and (9-12(l_{15}), 10-12(l_{17})), respectively as the 7th and 8th critical lines. In other words, the Jaccard similarity index (JSI) for these two sets of lines is 0.6 and the average JSI is 0.9 for this test case.

The effects of reactive power, losses, etc. are more highlighted in a network under stress (not in IEEE 24-bus [52]). So, IEEE 57-bus is selected as the second test case to compare both models. Figure 6 shows that the objective function (LS) of the previous method in all simulations are lower/equal and so, optimistic compared to the proposed AC-based approach. It presents the fact that restricting the available degrees of freedom (e.g., fixing voltages in DC-based method) makes the solution less optimal and accurate [34]. Furthermore, the DC-proposed critical lines are tested with ACOPF. The results show that the critical lines are not the real critical lines. This phenomenon has clearly happened when *k* is 4 and 5. Figure 7 also shows five worst-case load shedding scenarios (*k*=1 to 5) and their related lines based on both models. In this network, the average JSI is about 0.6. Note that thanks to the proposed approach the calculated load shedding is more accurate (with the same *k* presents more damage) and also, it provides more precise information about the critical lines that is vital for planning and remedial actions.

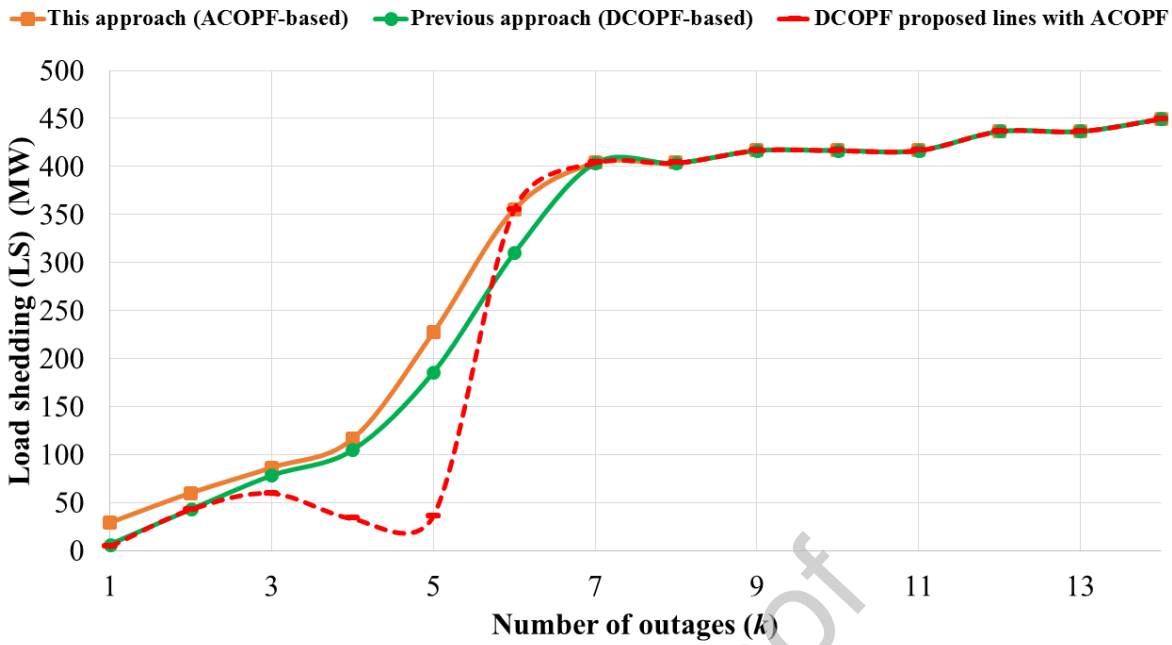

Figure 6. Load shedding for IEEE 57-bus as a function of number of outages (k).

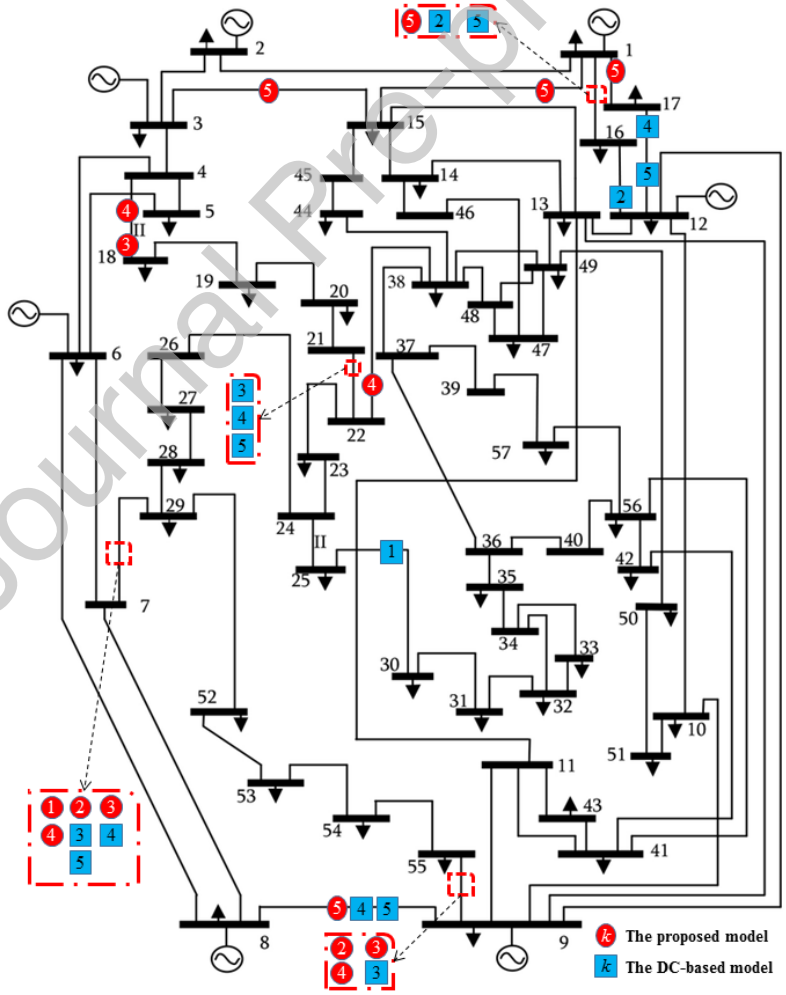

Figure 7. The IEEE 57-bus and optimal solutions for *k*=1 to 5 using both models.

5.3. Multi-period contingency analysis with daily peak loads

The system daily peak load of the IEEE RTS network (Figure 4) is used in the model to find out the effects of contingencies over a range of system demand levels (Figure 8). It should be noted when all lines are out of service, the system operator is forced to shed 1607 MW which is 56% of total demands. The remainders are directly connected to the generators' buses. The method determined that this total possible system load is shed with only 13 simultaneous outages. In addition, the results show that the maximum damage is in midweek of the high-demand season while the minimum load shedding is on weekends of the low-demand season. The maximum damages sometimes don't change significantly with the increase of the outages e.g., maximum load shedding of *N*-7 comparing with *N*-8 or change significantly e.g., maximum load shedding of *N*-4 comparing with *N*-5 (68% increase). This point is very important in the intentional attack-based studies where the interdiction resources are limited. Last but not least, this network is not *N*-1 secure. However, it occurs only on the 352nd day of the year (see Figure 4). This is a hidden *N*-1 contingency using the previous approaches [23, 53] because the main reason is the dominant flow of reactive power in that area (lines connected to bus 6). Hence, the proposed approach helps the decision makers of the energy sector for long-term operation planning in the power system.

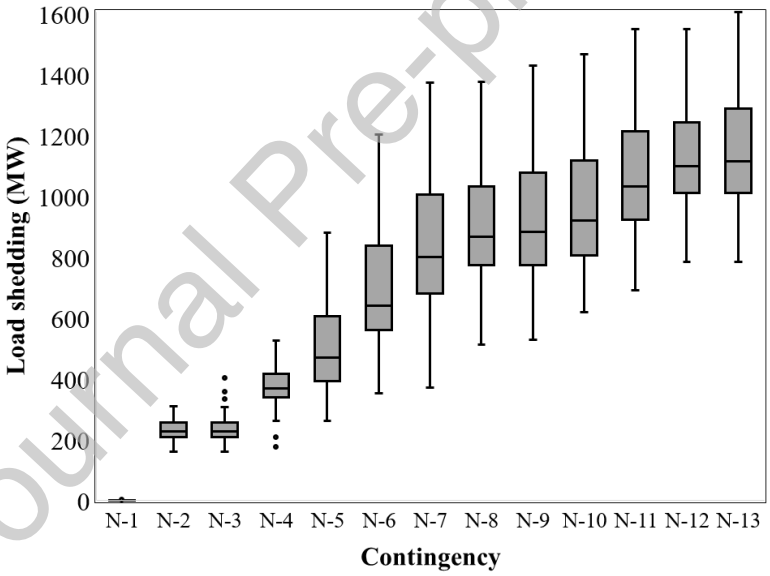

Figure 8. Effects of the contingencies with daily peak loads.

5.4. Multi-period contingency analysis with hourly peak loads

In the next step, this analysis is conducted similarly for the hourly peak loads of the 352nd day when the demands are the daily peak load of the year. Figure 9 shows the distribution of load shedding for the hourly peak loads of the 352nd day. The results show that the maximum damage is at around 5 to 7 p.m. while the minimum load shedding is at around 3 to 5 a.m. during the night. It is interesting to note that based on the used hourly peak loads, this network is not *N*-1 secure for hours between 4-7 p.m. when the hourly load profile (see Figure 4) has a peak. This information is essential for the decision makers of power system security sectors and operators making a robust and fast remedial action to protect the power

system. Furthermore, operators can use this approach for a day- ahead steady- state security assessment.

The model allows having critical lines for each contingency and time. Table 2 presents the critical lines and the consequences when the demand for the buses is the annual peak load. In this topology, the critical lines are the lines removing them leads isolating load buses in low-order contingencies (e.g., Figure 10 (a)). With increasing *k*, the model tries to separate the generation zone from the load zone. The generation zone of this topology is in 230 kV area where the generation capacity is much more than the required demands. Figure 10 (b) shows that the lines l_7, l_{21}, l_{22}, and l_{23} are the critical lines where removing them separates two zones. In the higher order of contingency, the model suggests removing all of the efficacious lines between generation buses and demands. The efficacious lines are the lines that removing them increases the load shedding. For instance, line 27 in Figure 10 (c) is not effective because the demand is much more than the generation capacity in bus n_{15}. On the contrary, bus n_{18} has much more generation capacity than the demand in the generation zone of Figure 10 (c). Therefore, removing lines in that zone is not effective. To summarize the results, according to the simulation results, the potential critical lines are radial lines (e.g., l_{11}), parallel lines (e.g., l_{25} and l_{26}, l_{36}, and l_{37}) and the lines connecting the generation to demand zones in a nearly centralized generation such as IEEE RTS.

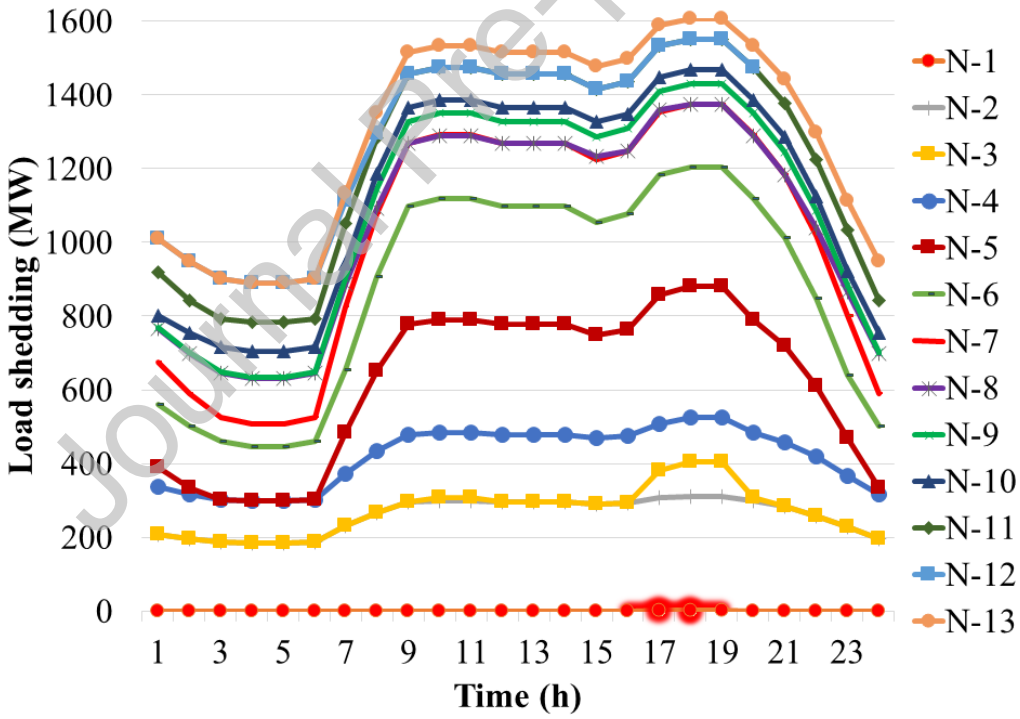

Figure 9. Effects of the contingencies with hourly peak loads.

Table 2. Outcomes of the proposed model when the demand of the buses is the annual peak load.

k	Critical lines	Load shedding (MW)	Simulation time (Min)
1	l_{10}	2	0.03
2	l_{29}, $(l_{36}, l_{37})^*$	309	0.19
3	l_{11}, $(l_{25}, l_{26})^*$, l_{28}	405	0.47
4	l_7, l_{21}, l_{22}, l_{23}	526	3.66
5	l_{21}, l_{22}, $(l_{25}, l_{26})^*$, l_{28}, $(l_{36}, l_{37})^*$	883	2.60
6	l_{18}, l_{20}, l_{21}, $(l_{25}, l_{26})^*$, l_{28}, $(l_{36}, l_{37})^*$	1204	3.25
7	l_{11}, l_{18}, l_{20}, l_{21}, $(l_{25}, l_{26})^*$, l_{28}, $(l_{36}, l_{37})^*$	1374	2.82
8	l_3, l_{11}, l_{18}, l_{20}, l_{21}, $(l_{25}, l_{26})^*$, l_{28}, $(l_{36}, l_{37})^*$	1377	1.80
9	l_{11}, l_{18}, l_{20}, l_{21}, l_{23}, l_{24}, $(l_{25}, l_{26})^*$, l_{29}, $(l_{36}, l_{37})^*$	1430	2.22
10	l_1, l_4, l_5, l_{11}, l_{15}, l_{17}, l_{18}, $(l_{25}, l_{26})^*$, l_{28}, $(l_{36}, l_{37})^*$	1469	1.11
11	l_2, l_3, l_4, l_5, l_{11}, l_{15}, l_{17}, l_{18}, $(l_{25}, l_{26})^*$, l_{28}, $(l_{36}, l_{37})^*$	1552	1.07
12	l_2, l_3, l_4, l_5, l_{11}, l_{18}, l_{20}, l_{21}, $(l_{25}, l_{26})^*$, l_{28}, l_{29}, $(l_{36}, l_{37})^*$	1552	0.60
13	l_2, l_3, l_4, l_5, l_{11}, l_{15}, l_{17}, l_{18}, l_{23}, l_{24}, $(l_{25}, l_{26})^*$, l_{29}, $(l_{36}, l_{37})^*$	1607	0.16

* The lines in the parentheses are the parallel lines between two nodes.

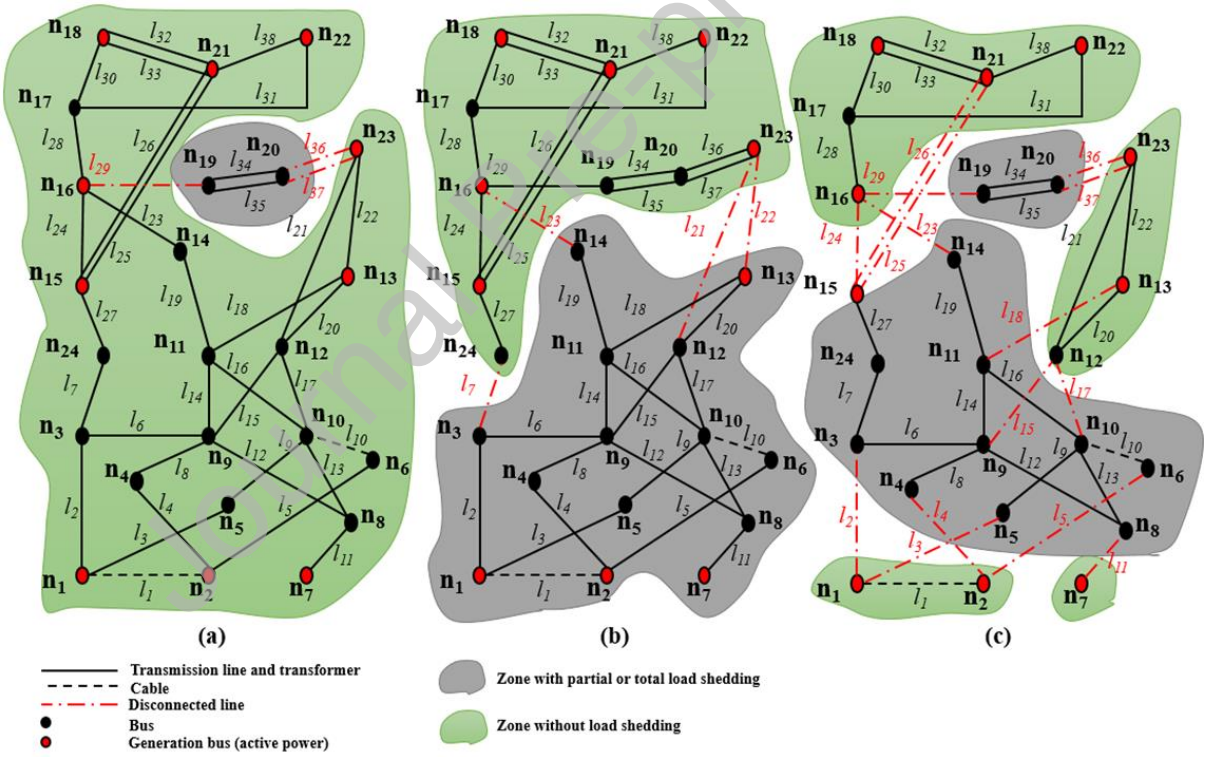

Figure 10. Topology of IEEE RTS under different contingencies, (a) *N*-2 (b) *N*-4 (c) *N*-13.

6. Discussions and future works

The main aim of this paper is to develop an approximation model of the original non-convex bilevel MINLP problem that is NP-hard and computationally challenging. The original problem includes an upper level whose objective is to identify exactly *k* components to maximize the damage (i.e. load shedding) in the system and a lower level whose objective is

mitigating the impacts of attacks and minimizing the damage consequences using ACOPF. We have not done any approximation for the upper-level problem. So, the upper-level solution of the approximation model is also valid for the original problem. The main approximation is performed in the lower-level problem where we used the duality theory and some proposed linearization techniques to replace it with a linear problem (LP).

Then, the accuracy of this approximation in the lower-level problem is investigated. First, the linearized ACOPF problem has been validated using an open-source software i.e., MATPOWER (see section 5.1). As the DCOPF problem is a simple version of ACOPF, deriving the DC-based approach from our proposed model is quite straightforward (see section 5.2). Then, these two problems are modelled with the same input and assumptions which ensures a fair comparison.

Our one-level MILP problem allows the use of high performance, efficient and reliable algorithm as well as off-the-shelf solvers such as Cplex to the desired precision level instead of employing a non-linear solver that does not guarantee to have a global optimum solution [19]. As our model is an approximation, the resultant solution is not necessarily the same as the global solution of the original bilevel MINLP problem but it will be very close when our approximation assumptions are valid (see section 2). Another application of the proposed model is to use it as a warm-start strategy to solve the original bilevel MINLP problem using a probable direct solution or metaheuristic algorithms. Exploring these ideas can be considered as good future extensions of our work.

In this paper, the *2M* piecewise linear (PWL) blocks and the *n*-sided convex regular polygon are used for the approximation of nonlinear terms in the lower-level problem. The accuracy of our model can be improved by adding more linear terms (i.e., *n* and *M*). Noted, the linearization technique for the quadratic function (i.e. PWL) does not need any binary variables given small voltage angles [42] which makes it much more tractable as compared to other linearization techniques which use either binary variables in their formulations [43] or the special ordered set of type 2 (SOS2) [36]. A large *M* or *n* improves the accuracy but increases the number of equations and accordingly the computational burden. Furthermore, a small *n* enforces more restrictions on transmission line capacity and might lead to the problem infeasibility. We set the linear terms based on the recommendations in [19, 36] for our test cases. Finding an optimal value of linear terms for a large-scale power system is good future work.

Our proposed model is a steady-state security model and a multi-period scenario is considered where typically, the highest load demand forecast is used in each time period. Dynamic modeling, implementing the uncertainty of the loads and generations, and robust assessment of uncertainty are other interesting topics that can be explored in our future work.

7. Conclusion

A novel multi-period AC-based approach is presented to analyze *N-k* contingencies in order to enhance the resilience of a bulk power system under multiple outages. This method is based on the Stackelberg game theory which includes an upper level whose objective is to identify exactly *k* components to maximize the damage (load shedding) in the system and a

lower level whose objective is mitigating the impacts of attacks and minimizing the damage consequences. Unlike the literature, in order to provide a more precise and real picture of the reactive power flow, losses as well as voltage profile, ACOPF is used in the lower-level problem as the operator's (defender's) tool. The resulting formulated problem is an AC-based bilevel MINLP problem in each time. To guarantee a globally optimal solution, The formulated problem is linearized and recast to the one-level MILP problem using the linearization techniques and the duality theory. The linearized ACOPF shows a very small error of 0.3% by assuming the predefined linearization parameters i.e., M=80 and n=64. The multi-period analysis is conducted with hourly and daily peak loads of the IEEE RTS. The method presents load shedding and the critical lines for each contingency over a range of system demand levels of this test system. Furthermore, the results show that in the congested systems especially where the reactive power flows predominate on some lines or buses such as cables or bus 6 in this case, the assessment cannot be adequately conducted only by the active power flows.

Appendix

To linearize equations (6) and (7), the practical assumptions are assumed for all buses. (i.e., the phase differences between the bus voltages are too small and the voltage magnitude is close to 1 p.u.). Then, the first-order approximation of Taylor's series with respect to the variables $\{V_i, V_j, c_{ij}, n_{ij}\}$ is used as follows:

$$P_{ij} \overset{\lambda_l}{=} z_l \left(G_{ij} \left(2V_i - 1 \right) - G_{ij} \left(V_i + V_j + c_{ij} - 2 \right) - B_{ij} n_{ij} \right) \tag{35}$$

$$Q_{ij} \overset{\mu_l}{=} z_l \left(-B_{ij} \left(2V_i - 1 \right) + B_{ij} \left(V_i + V_j + c_{ij} - 2 \right) - G_{ij} n_{ij} \right) \tag{36}$$

Where, $c_{ij} = \cos\theta_{ij} = 1 - \frac{(\theta_i - \theta_j)^2}{2}$ and $n_{ij} = \sin\theta_{ij} = \theta_i - \theta_j$. Then, the quadratic function linearized based on the proposed method in [42] by using 2M piecewise linear (PWL) blocks as below:

$$c_{ij} = 1 - \frac{(\theta_i - \theta_j)^2}{2} \overset{\chi_{ij}}{=} 1 - \frac{\sum_{m=1}^{M} ((2m-1)\Delta\theta_{ij})\theta_{ijm}}{2}; \quad m = 1 \cdots M, \forall i, j \in N \tag{37}$$

$$n_{ij} = \theta_i - \theta_j \overset{\xi_{ij}}{=} \delta_{ij}^{+} - \delta_{ij}^{-}; \quad \forall i, j \in N \tag{38}$$

$$n_{ij} \overset{\varepsilon_{ij}}{=} -n_{ji}; \quad \forall i, j \in N \tag{39}$$

In order to linearize the product of binary and continuous dual variables ($z_l\lambda_l$ and $z_l\mu_l$) in equations (21), (25)-(27). This product can be easily linearized using two sets of continuous variables T_l and H_l [27, 45]. For instance, $T_l = z_l\lambda_l$ can be linearized as follows:

$$
\begin{aligned}
&T_l = \lambda_l - H_l \\
&-Bz_l \le T_l \le Bz_l \\
&-B(1-z_l) \le H_l \le B(1-z_l)
\end{aligned} \tag{40}
$$

Where, B has to be big enough so that if $z_l = 0 (or 1)$, the inequalities of equation (40) would be nonbinding constraints. Equation (40) shows when $z_l = 1$, T_l will be equal to λ_l. Otherwise, T_l will be equal to zero.

Declaration of interests

☒ The authors declare that they have no known competing financial interests or personal relationships that could have appeared to influence the work reported in this paper.

Acknowledgment

The authors thank the anonymous referees for the precious comments, which have enabled significant improvements to the paper.

References

1. Cuadra, L., et al., *A Critical Review of Robustness in Power Grids Using Complex Networks Concepts.* Energies, 2015. **8**(9): p. 9211-9265.
2. Ferrario, E., N. Pedroni, and E. Zio, *Evaluation of the robustness of critical infrastructures by Hierarchical Graph representation, clustering and Monte Carlo simulation.* Reliability Engineering & System Safety, 2016. **155**: p. 78-96.
3. Scaparra, M.P. and R.L. Church, *A bilevel mixed-integer program for critical infrastructure protection planning.* Computers & Operations Research, 2008. **35**(6): p. 1905-1923.
4. Faramondi, L., et al., *Network Structural Vulnerability: A Multiobjective Attacker Perspective.* IEEE Transactions on Systems Man Cybernetics-Systems, 2019. **49**(10): p. 2036-2049.
5. Marrone, S., et al., *Vulnerability modeling and analysis for critical infrastructure protection applications.* International Journal of Critical Infrastructure Protection, 2013. **6**(3-4): p. 217-227.
6. Yang, Y.F., X.H. Guan, and Q.Z. Zhai, *Fast Grid Security Assessment With N-k Contingencies.* IEEE Transactions on Power Systems, 2017. **32**(3): p. 2193-2203.
7. (NERC), N.A.R.C., *NERC: Evaluation of Criteria, Methods, and Practices Used for System Design, Planning, and Analysis Response to NERC Blackout Recommendation 13c.* . 2019.
8. Sundar, K., et al., *Probabilistic N-k failure-identification for power systems.* Networks, 2018. **71**(3): p. 302-321.
9. Kaplunovich, P. and K. Turitsyn, *Fast and Reliable Screening of N-2 Contingencies.* IEEE Transactions on Power Systems, 2016. **31**(6): p. 4243-4252.
10. Fan, N., R. Chen, and J. Watson. *N-1-1 contingency-constrained optimal power flow by interdiction methods*. in *2012 IEEE Power and Energy Society General Meeting*. 2012.

11. Chatterjee, D., et al. *N-1-1 AC contingency analysis as a part of NERC compliance studies at midwest ISO*. in *Transmission and Distribution Conference and Exposition, 2010 IEEE PES*. 2010.
12. Abdi-Khorsand, M., M. Sahraei-Ardakani, and Y.M. Al-Abdullah, *Corrective Transmission Switching for N-1-1 Contingency Analysis.* IEEE Transactions on Power Systems, 2017. **32**(2): p. 1606-1615.
13. Abedi, A., et al., *MCDM approach for the integrated assessment of vulnerability and reliability of power systems.* IET Generation, Transmission & Distribution, 2019. **13**(20): p. 4741-4746.
14. Dolan, M., et al., *Forensic Disaster Analysis of Flood Damage at Commercial and Industrial Firms*, in *Flood Damage Survey and Assessment*. 2017, John Wiley & Sons, Inc. p. 195-209.
15. Kundak, S., *Cascading and unprecedented effects of disasters in urban system*, in *Intelligent Systems and Decision Making for Risk Analysis and Crisis Response*. 2013, CRC Press. p. 743-748.
16. Pascale, S., F. Sdao, and A. Sole, *A model for assessing the systemic vulnerability in landslide prone areas.* Natural Hazards and Earth System Sciences, 2010. **10**(7): p. 1575-1590.
17. Veen, A.V.D. and C. Logtmeijer, *Economic Hotspots: Visualizing Vulnerability to Flooding.* Natural Hazards, 2005. **36**(1): p. 65-80.
18. Abedi, A., L. Gaudard, and F. Romerio-Giudici, *Review of major approaches to analyze vulnerability in power system.* Reliability Engineering and System Safety, 2019. **183**: p. 153-172.
19. Akbari, T. and M.T. Bina, *Linear approximated formulation of AC optimal power flow using binary discretisation.* IET Generation Transmission & Distribution, 2016. **10**(5): p. 1117-1123.
20. Salmeron, J., K. Wood, and R. Baldick, *Analysis of electric grid security under terrorist threat.* IEEE Transactions on Power Systems, 2004. **19**(2): p. 905-912.
21. Sinha, A., P. Malo, and K. Deb, *A Review on Bilevel Optimization: From Classical to Evolutionary Approaches and Applications.* IEEE Transactions on Evolutionary Computation, 2018. **22**(2): p. 276-295.
22. Stackelberg, H.v., *The theory of the market economy*. 1952, New York,: Oxford University Press.
23. Arroyo, J.M. and F.D. Galiana, *On the solution of the bilevel programming formulation of the terrorist threat problem.* IEEE Transactions on Power Systems, 2005. **20**(2): p. 789-797.
24. Motto, A.L., J.M. Arroyo, and F.D. Galiana, *A mixed-integer LP procedure for the analysis of electric grid security under disruptive threat.* IEEE Transactions on Power Systems, 2005. **20**(3): p. 1357-1365.
25. Arroyo, J.M., *Bilevel programming applied to power system vulnerability analysis under multiple contingencies.* IET Generation Transmission & Distribution, 2010. **4**(2): p. 178-190.
26. Brown, G., et al., *Defending Critical Infrastructure.* INFORMS Journal on Applied Analytics, 2006. **36**(6): p. 530-544.
27. Alguacil, N., A. Delgadillo, and J.M. Arroyo, *A trilevel programming approach for electric grid defense planning.* Computers & Operations Research, 2014. **41**: p. 282-290.
28. Wu, X. and A.J. Conejo, *An Efficient Tri-Level Optimization Model for Electric Grid Defense Planning.* IEEE Transactions on Power Systems, 2017. **32**(4): p. 2984-2994.

29. Fang, Y.-P. and E. Zio, *An adaptive robust framework for the optimization of the resilience of interdependent infrastructures under natural hazards.* European Journal of Operational Research, 2019. **276**(3): p. 1119-1136.
30. Fang, Y.P., G. Sansavini, and E. Zio, *An Optimization-Based Framework for the Identification of Vulnerabilities in Electric Power Grids Exposed to Natural Hazards.* Risk Analysis, 2019. **39**(9): p. 1949-1969.
31. Che, L., et al., *A Mixed Integer Programming Model for Evaluating the Hidden Probabilities of N-k Line Contingencies in Smart Grids.* IEEE Transactions on Smart Grid, 2019. **10**(1): p. 1036-1045.
32. Nemati, H., M.A. Latify, and G.R. Yousefi, *Tri-level transmission expansion planning under intentional attacks: virtual attacker approach - part I: formulation.* IET Generation Transmission & Distribution, 2019. **13**(3): p. 390-398.
33. Nemati, H., M.A. Latify, and G.R. Yousefi, *Tri-level transmission Expansion planning under intentional attacks: virtual attacker approach-part II: case studies.* IET Generation Transmission & Distribution, 2019. **13**(3): p. 399-408.
34. Grigsby, L.L., *Power system stability and control*. 2016: CRC press.
35. Kim, T., et al., *Analyzing Vulnerability of Power Systems with Continuous Optimization Formulations.* IEEE Transactions on Network Science and Engineering, 2016. **3**(3): p. 132-146.
36. Arabpour, A., M.R. Besmi, and P. Maghouli, *Transmission Expansion Planning with Linearized AC Load Flow by Special Ordered Set Method.* Journal of Energy Engineering, 2018. **144**(2).
37. Karimi, S., P. Musilek, and A.M. Knight, *Dynamic thermal rating of transmission lines: A review.* Renewable & Sustainable Energy Reviews, 2018. **91**: p. 600-612.
38. Frank, S., J. Sexauer, and S. Mohagheghi, *Temperature-Dependent Power Flow.* IEEE Transactions on Power Systems, 2013. **28**(4): p. 4007-4018.
39. Soroudi, A., *Power system optimization modeling in GAMS*. Vol. 78. 2017: Springer.
40. Akbari, T. and M.T. Bina, *A linearized formulation of AC multi-year transmission expansion planning: A mixed-integer linear programming approach.* Electric Power Systems Research, 2014. **114**: p. 93-100.
41. Matoušek, J. and B. Gärtner, *Understanding and using linear programming*. Universitext. 222 p.
42. Motto, A.L., et al., *Network-constrained multiperiod auction for a pool-based electricity market.* IEEE Transactions on Power Systems, 2002. **17**(3): p. 646-653.
43. Pereira, M.V., et al., *Strategic bidding under uncertainty: A binary expansion approach.* IEEE Transactions on Power Systems, 2005. **20**(1): p. 180-188.
44. Akbari, T. and M.T. Bina, *Approximated MILP model for AC transmission expansion planning: global solutions versus local solutions.* IET Generation Transmission & Distribution, 2016. **10**(7): p. 1563-1569.
45. Floudas, C.A., *Nonlinear and mixed-integer optimization: fundamentals and applications*. 1995: Oxford University Press.
46. Christie, R. and I. Dabbagchi, *IEEE 57-Bus System.* 1993.
47. Grigg, C., et al., *The IEEE Reliability Test System-1996. A report prepared by the Reliability Test System Task Force of the Application of Probability Methods Subcommittee.* IEEE Transactions on Power Systems, 1999. **14**(3): p. 1010-1020.
48. Zimmerman, R.D., C.E. Murillo-Sanchez, and R.J. Thomas, *MATPOWER: Steady-State Operations, Planning, and Analysis Tools for Power Systems Research and Education.* IEEE Transactions on Power Systems, 2011. **26**(1): p. 12-19.

49. Anghilante, R., et al., *Innovative power-to-gas plant concepts for upgrading of gasification bio-syngas through steam electrolysis and catalytic methanation.* Energy Conversion and Management, 2019. **183**: p. 462-473.
50. Saadat, H., *Power system analysis*. 1999, Boston: WCB/McGraw-Hill. 697 pages.
51. Cetinay, H., et al., *Comparing the Effects of Failures in Power Grids under the AC and DC Power Flow Models.* IEEE Transactions on Network Science and Engineering, 2018: p. 1-1.
52. Nagarajan, R. and C. Singh. *Multi-area reliability evaluation using composite system framework*. in *2016 IEEE International Conference on Power System Technology (POWERCON)*. 2016.
53. Abedi, A., L. Gaudard, and F. Romerio, *Power flow-based approaches to assess vulnerability, reliability, and contingency of the power systems: The benefits and limitations.* Reliability Engineering & System Safety, 2020. **201**: p. 106961.